

Supplementary Materials for
Sliding ferroelectricity in bilayer phosphorus-analogue compounds:
mechanisms and applications

Dong-Dong Wang,^a Xin-Yi Gao,^a Yan-Dong Guo,^{*a} Yu-Ting Guo,^a Zhi-Peng Huan,^a Li-Yan Lin,^a Yue Jiang,^{*b} Zeng-Yun Gu,^a Hong-Li Zeng,^{*c} Xiao-Hong Yan^c

^aCollege of Electronic and Optical Engineering, Nanjing University of Posts and Telecommunications, Nanjing 210046, China. E-mail: yandongguo@njupt.edu.cn

^bCollege of Science, Jinling Institute of Technology, Nanjing 211169, China. E-mail: jiangyue@jit.edu.cn

^cCollege of Natural Science, Nanjing University of Posts and Telecommunications, Nanjing 210046, China. E-mail: hlzeng@njupt.edu.cn

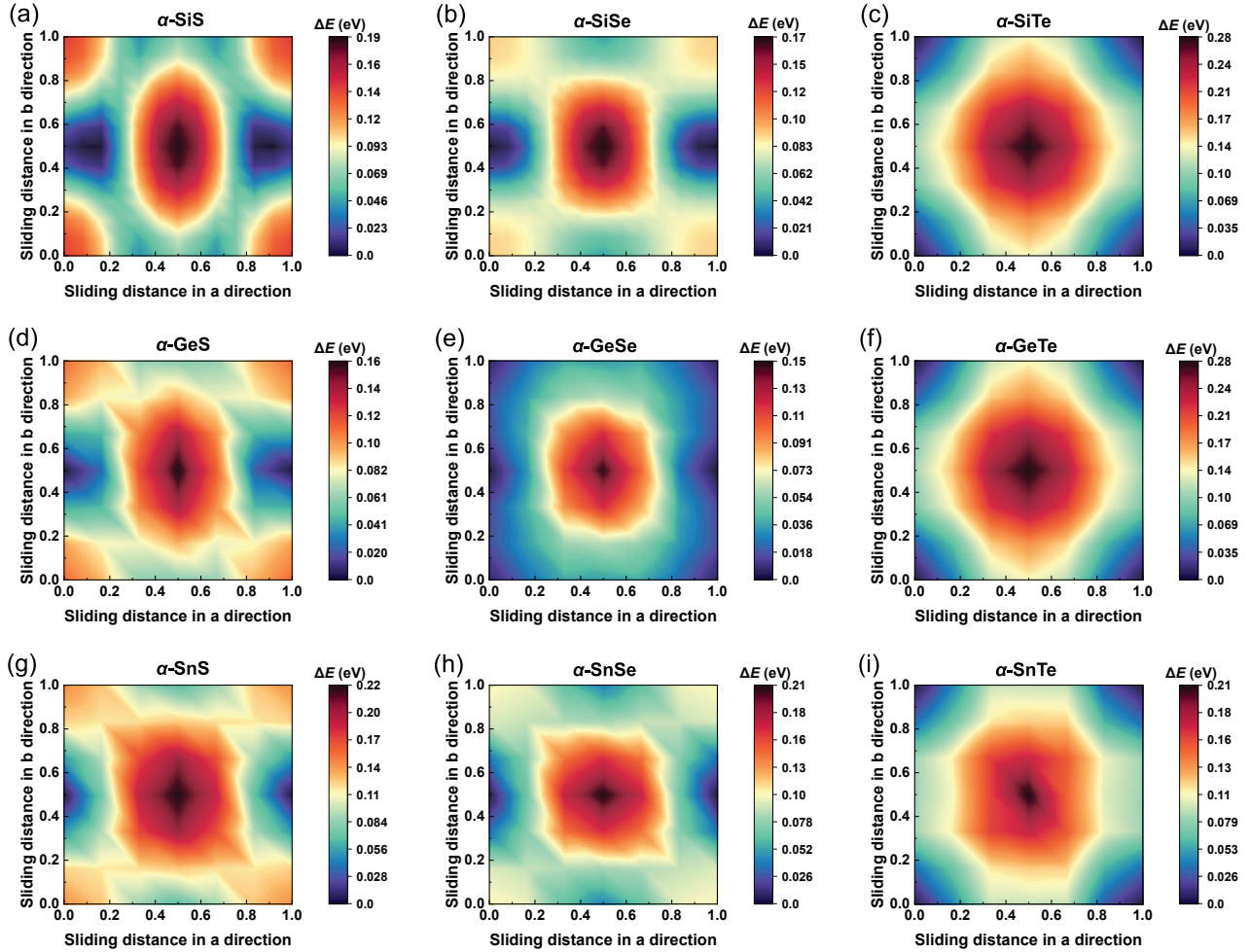


Fig. S1 (a)-(i) The energy profiles of the sliding bilayer α -phase MX materials ($M = \text{Si, Ge, and Sn}; X = \text{S, Se, and Te}$). Among these materials, only the bilayer $\alpha\text{-SiS}$ exhibits a clear double well sliding path.

Table S1 Lattice constant, ferroelectric switching barrier (E_b) and out-of-plane polarization (P_{out}) of MX materials ($M = \text{Si, Ge, Sn, and Pb}; X = \text{S, Se, and Te}$).

Configuration	Lattice constant (\AA)	E_b (meV/u.c.)	P_{out} (pC/m)
bilayer $\alpha\text{-SiS}$	4.32/4.10	7.8	5.6
bilayer $\beta\text{-SiS}$	3.30	3.89	0.28
bilayer $\beta\text{-SiSe}$	3.50	5.50	0.38
bilayer $\beta\text{-SiTe}$	3.82	7.50	0.55
bilayer $\beta\text{-GeS}$	3.48	4.70	0.28
bilayer $\beta\text{-GeSe}$	3.65	6.55	0.33
bilayer $\beta\text{-GeTe}$	3.94	8.85	0.55
bilayer $\beta\text{-SnS}$	3.73	6.17	0.1
bilayer $\beta\text{-SnSe}$	3.91	8.84	0.2
bilayer $\beta\text{-SnTe}$	4.16	11.14	0.5
bilayer $\beta\text{-PbS}$	3.94	9.56	0.08
bilayer $\beta\text{-PbSe}$	4.06	12.10	0.13
bilayer $\beta\text{-PbTe}$	4.30	14.20	0.53

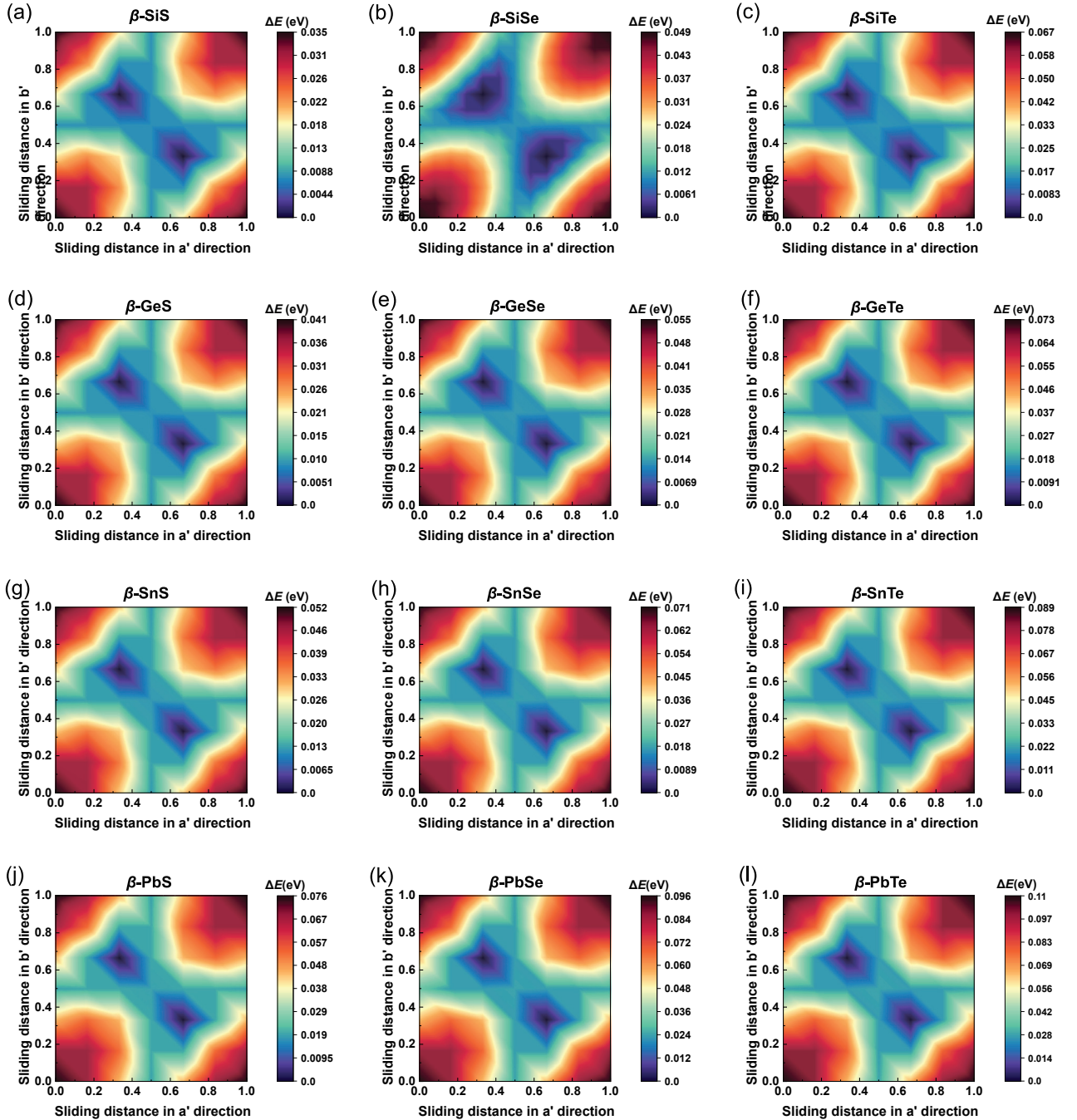


Fig. S2 (a)-(l) The energy profiles of the sliding bilayer β -phase MX materials ($M = \text{Si, Ge, Sn and Pb; } X = \text{S, Se, and Te}$). All materials exhibit distinct double potential energy well.

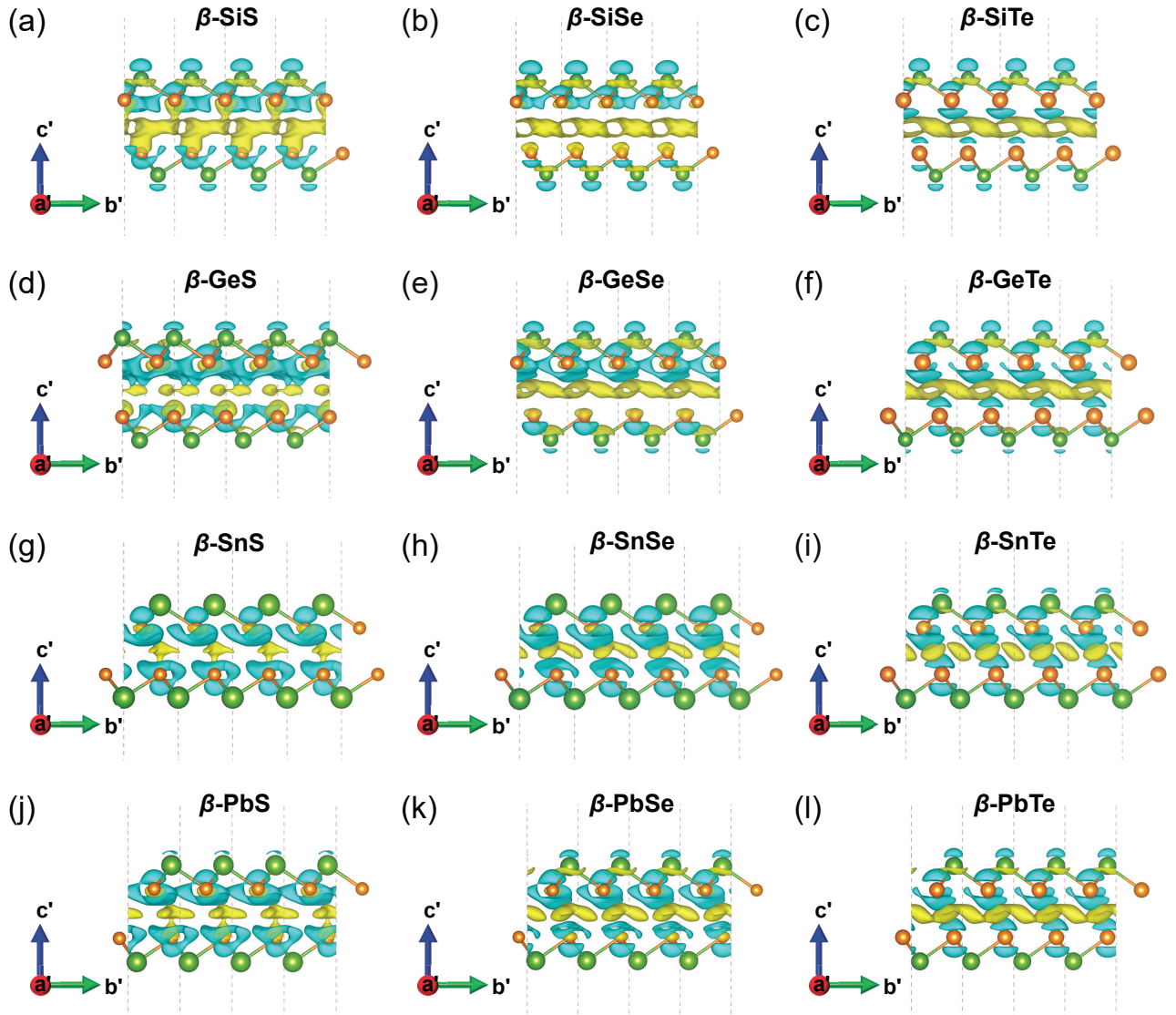


Fig. S3 (a)-(l) The differential charge density distributions of the maximum polarization in the MX materials ($M = \text{Si, Ge, Sn, and Pb}; X = \text{S, Se, and Te}$), where yellow indicates charge accumulation and blue indicates hole accumulation. When the M atom is fixed, with the increasing atomic number of X atom, the number of charges involved in interlayer transfer also increases significantly.

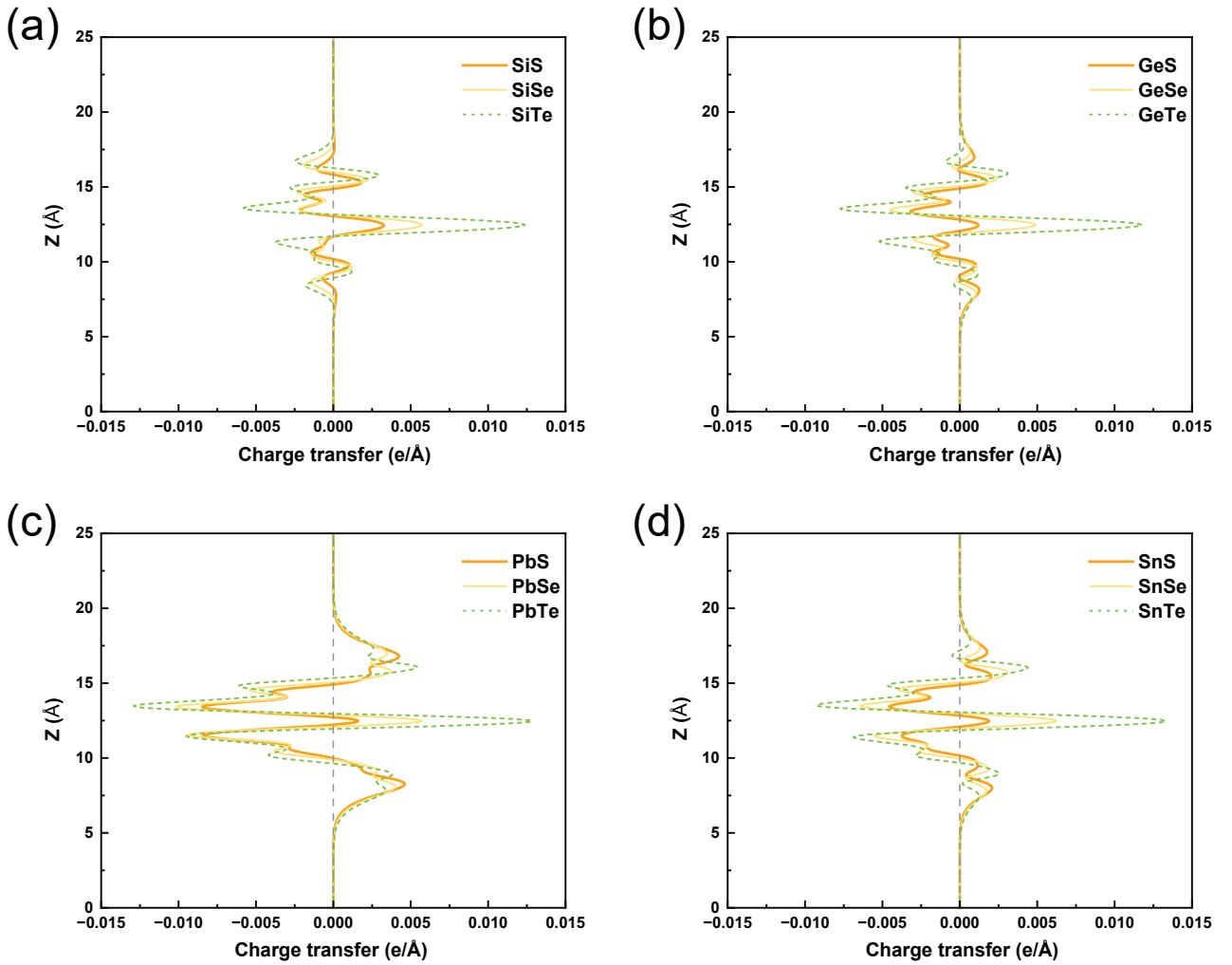


Fig. S4 (a)-(l) The planar differential charge density distributions of the maximum polarization in the MX materials ($\text{M} = \text{Si}, \text{Ge}, \text{Sn}, \text{and Pb}; \text{X} = \text{S}, \text{Se}, \text{and Te}$). By using contrast to highlight, as the atomic number of X atom increases, the overall amount of charge involved in charge transfer also increases.

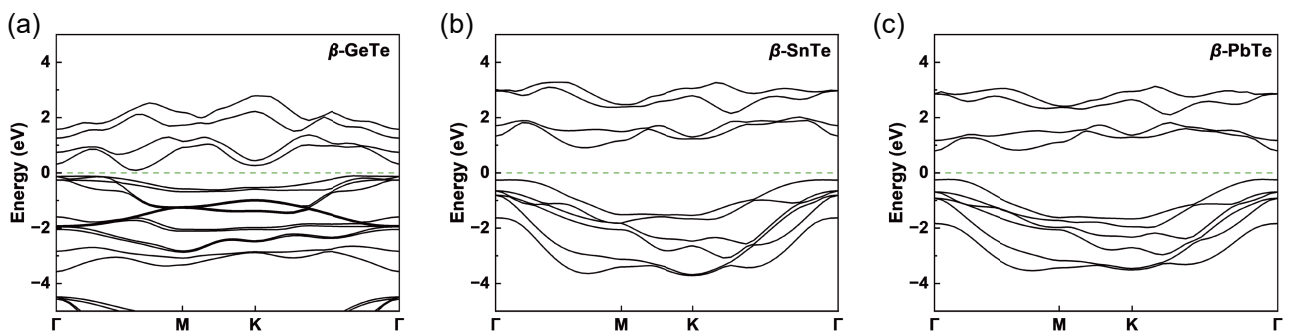


Fig. S5 (a)-(c) The band structure diagrams of $\beta\text{-GeTe}$, $\beta\text{-PbTe}$, and $\beta\text{-SnTe}$, which are used as channel materials.

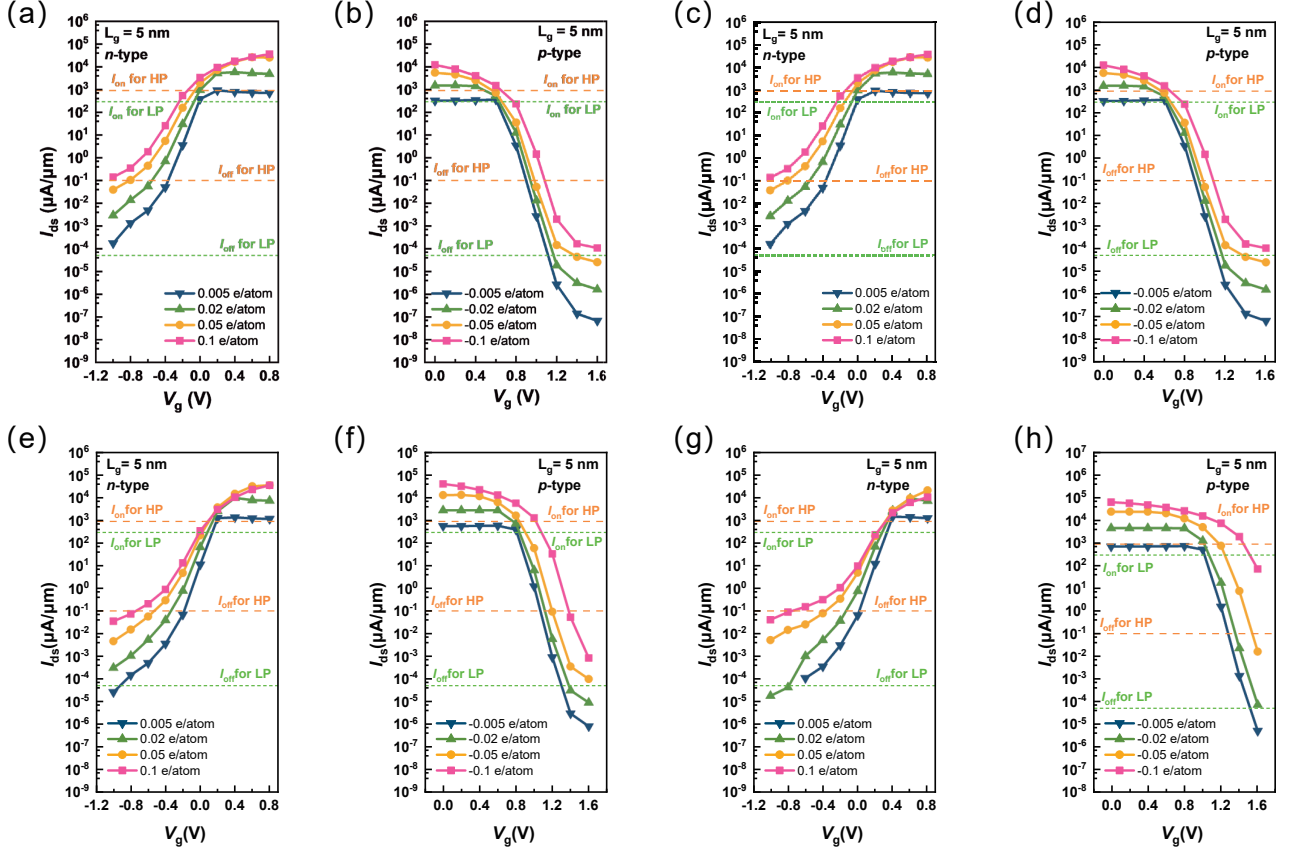


Fig. S6 (a)-(b) The doping concentration testing of bilayer α -SiS. (c)-(d) The doping concentration testing of bilayer β -SiTe. (e)-(f) The doping concentration testing of bilayer β -SnTe. (g)-(h) The doping concentration testing of bilayer β -PbTe. The black dashed lines represent the ITRS off-state current standards for high performance (HP) and low power (LP) devices, respectively.

Table S2 The device performance of the sub-5-nm-gate bilayer α -SiS FETs against the ITRS 2013 requirements for HP and LP application, including on-state current (I_{on}), off-state current (I_{off}) and on-off-ratio (I_{on}/I_{off}). The data in bold black indicates compliance with the ITRS standards, while the data represented by hyphens indicates that the curve struggles to reach the cutoff current.

Type	Expansion direction	L_g (nm)+UL(nm)	HP			LP		
			I_{on} ($\mu\text{A}/\mu\text{m}$)	I_{off} ($\mu\text{A}/\mu\text{m}$)	I_{on}/I_{off}	I_{on} ($\mu\text{A}/\mu\text{m}$)	I_{off} ($\mu\text{A}/\mu\text{m}$)	I_{on}/I_{off}
ITRS 2013								
n-type	along a direction	5+0	900.00	0.10	1.89E+04	-	-	-
n-type	along a direction	5+1	3189.46	0.10	3.19E+04	567.04	5E-5	1.13E+07
n-type	along a direction	5+2	2761.85	0.10	2.76E+04	888.98	5E-5	1.77E+07
n-type	along a direction	5+3	1878.52	0.10	1.88E+04	638.77	5E-5	1.27E+07
n-type	along a direction	3+0	-	-	-	-	-	-
n-type	along a direction	3+1	-	-	-	-	-	-
n-type	along a direction	3+2	1963.41	0.10	1.96E+04	-	-	-
n-type	along a direction	3+3	1293.07	0.10	1.29E+04	-	-	-
n-type	along a direction	1+0	-	-	-	-	-	-
p-type	along a direction	5+0	1187.24	0.10	1.18E+04	-	-	-
p-type	along a direction	5+1	2454.24	0.10	2.45E+04	0.01	5E-5	1.30E+02
p-type	along a direction	5+2	2321.13	0.10	2.32E+04	340.32	5E-5	6.80E+06
p-type	along a direction	5+3	738.98	0.10	7.38E+03	334.19	5E-5	6.60E+06
p-type	along a direction	3+0	-	-	-	-	-	-
p-type	along a direction	3+1	534.95	0.10	5.34E+03	-	-	-
p-type	along a direction	3+2	1180.43	0.10	1.18E+04	-	-	-
p-type	along a direction	3+3	878.07	0.10	8.78E+03	4.24	5E-5	8.48E+04
p-type	along a direction	1+0	-	-	-	-	-	-

Table S3 The device performance of the sub-5-nm-gate bilayer β -SiTe FETs against the ITRS 2013 requirements for HP and LP application, including on-state current (I_{on}), off-state current (I_{off}) and on-off-ratio (I_{on}/I_{off}). The data in bold black indicates compliance with the ITRS standards, while the data represented by hyphens indicates that the curve struggles to reach the cutoff current.

Type	Expansion direction	L_g (nm)+UL(nm)	HP			LP		
			I_{on} ($\mu\text{A}/\mu\text{m}$)	I_{off} ($\mu\text{A}/\mu\text{m}$)	I_{on}/I_{off}	I_{on} ($\mu\text{A}/\mu\text{m}$)	I_{off} ($\mu\text{A}/\mu\text{m}$)	I_{on}/I_{off}
ITRS 2013			900.00	0.10		295.00	5E-5	
n-type	along a direction	5+0	3417.69	0.10	3.42E+04	-	-	-
n-type	along a direction	5+1	5026.35	0.10	5.63E+04	-	-	-
n-type	along a direction	5+3	2329.51	0.10	2.23E+04	719.13	5E-5	1.44E+07
n-type	along a direction	5+5	916.99	0.10	9.17E+03	291.92	5E-5	5.84E+06
n-type	along a direction	3+0	-	-	-	-	-	-
n-type	along a direction	3+1	166.08	0.10	1.66E+03	-	-	-
n-type	along a direction	3+3	1967.96	0.10	1.97E+04	-	-	-
n-type	along a direction	3+5	739.04	0.10	7.39E+03	87.48	5E-5	1.75E+06
n-type	along a direction	1+0	-	-	-	-	-	-
n-type	along b direction	5+0	2380.46	0.10	2.38E+04	-	-	-
n-type	along b direction	5+1	5311.86	0.10	5.31E+04	-	-	-
n-type	along b direction	5+3	2189.99	0.10	2.19E+04	226.58	5E-5	4.53E+06
n-type	along b direction	5+5	848.95	0.10	8.49E+03	243.52	5E-5	4.87E+06
n-type	along b direction	3+0	-	-	-	-	-	-
n-type	along b direction	3+1	-	-	-	-	-	-
n-type	along b direction	3+3	3430.98	0.10	3.43E+04	-	-	-
n-type	along b direction	3+5	1512.03	0.10	1.51E+04	0.76	5E-5	1.52E+04
n-type	along b direction	1+0	-	-	-	-	-	-
p-type	along a direction	5+0	1647.56	0.10	1.65E+04	879.85	5E-5	1.76E+07
p-type	along a direction	5+1	1597.34	0.10	1.60E+04	750.03	5E-5	1.50E+07
p-type	along a direction	5+3	672.14	0.10	6.72E+03	291.08	5E-5	5.82E+06
p-type	along a direction	5+5	329.01	0.10	3.29E+03	-	-	-
p-type	along a direction	3+0	1498.10	0.10	1.50E+04	-	-	-
p-type	along a direction	3+1	1462.40	0.10	1.46E+04	348.04	5E-5	6.96E+06
p-type	along a direction	3+3	614.98	0.10	6.15E+03	255.69	5E-5	5.11E+06
p-type	along a direction	3+5	305.89	0.10	3.06E+03	138.20	5E-5	2.76E+06
p-type	along a direction	1+0	-	-	-	-	-	-
p-type	along b direction	5+0	1484.71	0.10	1.48E+04	889.62	5E-5	1.78E+07
p-type	along b direction	5+1	1462.13	0.10	1.46E+04	769.30	5E-5	1.54E+07
p-type	along b direction	5+3	634.35	0.10	6.34E+03	289.93	5E-5	5.80E+06
p-type	along b direction	5+5	310.64	0.10	3.11E+03	128.02	5E-5	2.56E+06
p-type	along b direction	3+0	2360.72	0.10	2.36E+04	-	-	-
p-type	along b direction	3+1	2625.63	0.10	2.62E+04	518.76	5E-5	1.04E+07
p-type	along b direction	3+3	941.67	0.10	9.42E+03	408.90	5E-5	8.18E+06
p-type	along b direction	3+5	474.78	0.10	4.75E+03	236.50	5E-5	4.73E+06
p-type	along b direction	1+0	-	-	-	-	-	-

Table S4 The device performance of the sub-5-nm-gate bilayer β -SnTe FETs against the ITRS 2013 requirements for HP and LP application, including on-state current (I_{on}), off-state current (I_{off}) and on-off-ratio (I_{on}/I_{off}). The data in bold black indicates compliance with the ITRS standards, while the data represented by hyphens indicates that the curve struggles to reach the cutoff current.

Type	Expansion direction	L_g (nm)+UL(nm)	HP			LP		
			I_{on} ($\mu\text{A}/\mu\text{m}$)	I_{off} ($\mu\text{A}/\mu\text{m}$)	I_{on}/I_{off}	I_{on} ($\mu\text{A}/\mu\text{m}$)	I_{off} ($\mu\text{A}/\mu\text{m}$)	I_{on}/I_{off}
ITRS 2013			900.00	0.10		295.00	5E-5	
n-type	along a direction	5+0	4227.00	0.10	4.23E+04	-	-	-
n-type	along a direction	5+1	4787.28	0.10	4.79E+04	36.02	5E-5	7.20E+05
n-type	along a direction	5+3	2136.27	0.10	2.14E+04	1187.34	5E-5	2.37E+07
n-type	along a direction	5+5	770.38	0.10	7.70E+03	518.20	5E-5	1.04E+07
n-type	along a direction	3+0	10.91	0.10	1.09E+02	-	-	-
n-type	along a direction	3+1	1086.89	0.10	1.09E+04	-	-	-
n-type	along a direction	3+3	1737.27	0.10	1.74E+04	4.37	5E-5	8.73E+04
n-type	along a direction	3+5	1259.89	0.10	1.26E+04	659.25	5E-5	1.32E+07
n-type	along a direction	1+0	-	-	-	-	-	-
n-type	along b direction	5+0	5123.68	0.10	5.12E+04	-	-	-
n-type	along b direction	5+1	6031.19	0.10	6.03E+04	0.39	5E-5	7.73E+03
n-type	along b direction	5+3	2524.02	0.10	2.52E+04	1082.62	5E-5	2.17E+07
n-type	along b direction	5+5	1040.30	0.10	1.04E+04	520.60	5E-5	1.04E+07
n-type	along b direction	3+0	-	-	-	-	-	-
n-type	along b direction	3+1	881.90	0.10	8.82E+03	-	-	-
n-type	along b direction	3+3	2297.39	0.10	2.30E+04	-	-	-
n-type	along b direction	3+5	2485.34	0.10	2.49E+04	1326.67	5E-5	2.65E+07
n-type	along b direction	1+0	-	-	-	-	-	-
p-type	along a direction	5+0	1544.27	0.10	1.54E+04	1207.42	5E-5	2.41E+07
p-type	along a direction	5+1	1559.89	0.10	1.56E+04	1077.46	5E-5	2.15E+07
p-type	along a direction	5+3	834.68	0.10	8.35E+03	371.08	5E-5	7.42E+06
p-type	along a direction	5+5	491.51	0.10	4.92E+03	-	-	-
p-type	along a direction	3+0	1422.49	0.10	1.42E+04	-	-	-
p-type	along a direction	3+1	1485.04	0.10	1.49E+04	-	-	-
p-type	along a direction	3+3	826.31	0.10	8.26E+03	305.26	5E-5	6.11E+06
p-type	along a direction	3+5	379.82	0.10	3.80E+03	176.76	5E-5	3.54E+06
p-type	along a direction	1+0	-	-	-	-	-	-
p-type	along b direction	5+0	1487.32	0.10	1.49E+04	1049.17	5E-5	2.10E+07
p-type	along b direction	5+1	1461.78	0.10	1.46E+04	1067.34	5E-5	2.13E+07
p-type	along b direction	5+3	775.61	0.10	7.76E+03	356.25	5E-5	7.12E+06
p-type	along b direction	5+5	363.22	0.10	3.63E+03	-	-	-
p-type	along b direction	3+0	1440.30	0.10	1.44E+04	-	-	-
p-type	along b direction	3+1	1444.49	0.10	1.45E+04	-	-	-
p-type	along b direction	3+3	767.39	0.10	7.67E+03	308.60	5E-5	6.17E+06
p-type	along b direction	3+5	361.19	0.10	3.61E+03	-	-	-
p-type	along b direction	1+0	-	-	-	-	-	-

Table S5 The device performance of the sub-5-nm-gate bilayer β -PbTe FETs against the ITRS 2013 requirements for HP and LP application, including on-state current (I_{on}), off-state current (I_{off}) and on-off-ratio (I_{on}/I_{off}). The data in bold black indicates compliance with the ITRS standards, while the data represented by hyphens indicates that the curve struggles to reach the cutoff current.

Type	Expansion direction	L_g (nm)+UL(nm)	HP			LP		
			I_{on} ($\mu\text{A}/\mu\text{m}$)	I_{off} ($\mu\text{A}/\mu\text{m}$)	I_{on}/I_{off}	I_{on} ($\mu\text{A}/\mu\text{m}$)	I_{off} ($\mu\text{A}/\mu\text{m}$)	I_{on}/I_{off}
ITRS 2013			900.00	0.10		295.00	5E-5	
n-type	along a direction	5+0	3388.01	0.10	3.39E+04	-	-	-
n-type	along a direction	5+1	3434.10	0.10	3.43E+04	-	-	-
n-type	along a direction	5+3	1529.83	0.10	1.53E+04	887.78	5E-5	1.78E+07
n-type	along a direction	5+5	540.81	0.10	5.41E+03	320.73	5E-5	6.41E+06
n-type	along a direction	3+0	22.70	0.10	2.27E+02	-	-	-
n-type	along a direction	3+1	823.13	0.10	8.23E+03	-	-	-
n-type	along a direction	3+3	1395.73	0.10	1.40E+04	-	-	-
n-type	along a direction	3+5	456.40	0.10	4.56E+03	195.98	5E-5	3.92E+06
n-type	along a direction	1+0	-	-	-	-	-	-
n-type	along b direction	5+0	4240.21	0.10	4.24E+04	-	-	-
n-type	along b direction	5+1	4834.59	0.10	4.83E+04	-	-	-
n-type	along b direction	5+3	2573.55	0.10	2.57E+04	1251.89	5E-5	2.50E+07
n-type	along b direction	5+5	999.78	0.10	1.00E+04	508.67	5E-5	1.02E+07
n-type	along b direction	3+0	1.94	0.10	1.94E+01	-	-	-
n-type	along b direction	3+1	706.57	0.10	7.07E+03	-	-	-
n-type	along b direction	3+3	1201.14	0.10	1.20E+04	-	-	-
n-type	along b direction	3+5	2397.92	0.10	2.40E+04	1286.66	5E-5	2.57E+07
n-type	along b direction	1+0	-	-	-	-	-	-
p-type	along a direction	5+0	2167.58	0.10	2.17E+04	1092.60	5E-5	2.19E+07
p-type	along a direction	5+1	2242.60	0.10	2.24E+04	1251.06	5E-5	2.50E+07
p-type	along a direction	5+3	1082.05	0.10	1.08E+04	423.18	5E-5	8.46E+06
p-type	along a direction	5+5	488.88	0.10	4.89E+03	146.00	5E-5	2.92E+06
p-type	along a direction	3+0	1462.20	0.10	1.46E+04	-	-	-
p-type	along a direction	3+1	2017.09	0.10	2.02E+04	-	-	-
p-type	along a direction	3+3	885.29	0.10	8.85E+03	297.16	5E-5	5.94E+06
p-type	along a direction	3+5	446.41	0.10	4.46E+03	147.76	5E-5	2.96E+06
p-type	along a direction	1+0	-	-	-	-	-	-
p-type	along b direction	5+0	2174.14	0.10	2.17E+04	1059.83	5E-5	2.12E+07
p-type	along b direction	5+1	2150.27	0.10	2.15E+04	1122.54	5E-5	2.25E+07
p-type	along b direction	5+3	1123.35	0.10	1.12E+04	508.01	5E-5	1.02E+07
p-type	along b direction	5+5	490.41	0.10	4.90E+03	242.35	5E-5	4.85E+06
p-type	along b direction	3+0	705.04	0.10	7.05E+03	-	-	-
p-type	along b direction	3+1	2082.52	0.10	2.08E+04	-	-	-
p-type	along b direction	3+3	942.49	0.10	9.42E+03	330.24	5E-5	6.60E+06
p-type	along b direction	3+5	476.58	0.10	4.77E+03	-	-	-
p-type	along b direction	1+0	-	-	-	-	-	-